measure the resonant Raman enhancement, it was necessary that the Raman intensities be at least comparable to the PL intensities. In the Raman sample, this condition was satisfied by using thin barriers to reduce the PL intensity. However, in other samples, such as the GaAs/$Al_{0.3}Ga_{0.7}As$ sample used for the NMR experiment, it was not possible to detect sufficient intensity enhancements on top of much stronger PL intensities, and we could not do Raman spectroscopy. In contrast to the Raman spectroscopy, the NMR was measured through changes in the PL energy. For this reason, the experiment benefits from a strongly luminescing sample. In both cases, the narrow spectral lines allowed us to resolve individual QDs, but in the NMR, because we were measuring changes in the Overhauser shifts, it was especially important to have very narrow PL spectral lines. Our spectral resolution (in other words, how well we can pick the resonance energy) is given roughly by the PL linewidth divided by the signal to noise ratio. Currently, this is about 5 μeV, and we can measure changes in nuclear polarization down to about 6%.

Previously, the most sensitive resonant Raman and optical NMR experiments performed on semiconductor nanostructures involved at least 10^9 nuclei (*11*, *16*). The current experiments represent an increase in sensitivity of five orders of magnitude. Recently, there has also been extensive effort in micro-Raman spectroscopy, including work at helium temperature (*17*), and there are pioneering efforts in optical-near-field Raman imaging at room temperature with lateral spatial resolutions down to 250 nm (*18*). It is important to note that, although the aperture sizes in our experiments were restricted to 200 nm or larger, the actual resolution of our experiments is much better because of our use of resonance techniques. By resonating with a single QD, we are probing the nuclei within that QD, and thus, our lateral spatial resolution is about 10 nm, an order of magnitude better than previous optical-near-field Raman spectroscopy. In some cases it should be possible to apply such resonance techniques to optical near-field imaging to enhance both sensitivity and selectivity.

There is no obvious reason why the experiments presented here could not be extended to smaller sizes or to other material systems. The present experiments demonstrate that if optical spectroscopy on single quantum units can be done, then nuclear spectroscopy on the same scale is possible.

REFERENCES AND NOTES

1. H. F. Hess, E. Betzig, T. D. Harris, L. N. Pfeiffer, K. W. West, *Science* **264**, 1740 (1994); K. Brunner, G. Abstreiter, G. Bohm, G. Trankle, G. Weimann, *Phys. Rev. Lett.* **73**, 1138 (1994); A. Zrenner *et al.*, *ibid.* **72**, 3382 (1994); W. Heller and U. Bockelmann, *Phys. Rev. B* **55**, R4871 (1997).
2. D. Gammon, E. S. Snow, D. S. Katzer, *Appl. Phys. Lett.* **67**, 2391 (1995).
3. D. Gammon, E. S. Snow, B. V. Shanabrook, D. S. Katzer, D. Park, *Science* **273**, 87 (1996).
4. _____ *Phys. Rev. Lett.* **76**, 3005 (1996).
5. S. W. Brown T. A. Kennedy, D. Gammon, E. S. Snow, *Phys. Rev B* **54**, R17339 (1996).
6. M. Nirmal *et al.*, *Nature* **383**, 802 (1996); S. A. Empedocles, D. J. Norris, M. G. Bawendi, *Phys. Rev. Lett.* **77**, 3873 (1996); S. A. Blanton, M. A. Hines, P. Guyot-Sionnest, *Appl. Phys. Lett.* **69**, 3905 (1996); Al. L. Efros and M. Rosen, *Phys. Rev. Lett.* **78**, 1110 (1997).
7. J. Kohler, A. C. J. Brouwer, E. J. J. Groenen, J. Schmidt, *Science* **268**, 1457 (1995); S. Nie and S. R. Emory, *ibid.* **275**, 1102 (1997); J. Wrachtrup, A. Gruber, L. Fleury, C. von Borczyskowski, *Chem. Phys. Lett.* **267**, 179 (1997).
8. For a review, see B. Jusserand and M. Cardona, in *Light Scattering in Solids V*, M. Cardona and G. Guntherodt, Eds. (Springer-Verlag, Heidelberg, 1989), pp. 49–152.
9. For a review, see D. Paget and V. L. Berkovits, in *Optical Orientation*, F. Meier and B. P. Zakharchenya, Eds. (North-Holland, New York, 1984), chap. 9.
10. We estimate 0.01 QDs μm^{-2} μeV^{-1} from the PL spectra at small apertures. This density gives about 300 QDs within the resonance linewidth in a 25-μm aperture.
11. D. Gammon, B. V. Shanabrook, D. S. Katzer, *Phys. Rev. Lett.* **67**, 1547 (1991).
12. There is convincing evidence that the structure at energies less than that of the LO_2 peak is primarily due to interface phonons mixed with confined phonons [A. J. Shields, M. P. Chamberlain, M. Cardona, K. Eberl, *Phys. Rev. B* **51**, 17728 (1995)].
13. The exciton is composed of an electron and a heavy hole, each of which has a spin degeneracy of 2. Of the four resulting combinations, only two are dipole-allowed and absorb or emit light. See, for example, H. W. van Kesteren, E. C. Cosman, W. A. J. A. van der Poel, C. T. Foxon, *Phys. Rev. B* **41**, 5283 (1990).
14. The longitudinal field must be larger than the dipole fields from neighboring nuclei (5 G) and large enough such that the magnetic Zeeman energy is greater than fine structure splitting arising from deviations from cylindrical symmetry (0.2 T) (*4*, *5*).
15. In the NMR measurements, the laser was tuned to the beginning of the 2D continuum about 10 meV above the QD spectral lines; therefore, a number of QDs were pumped simultaneously. The PL, however, probes individual QDs through the contact hyperfine interaction, which is a local interaction (*9*).
16. G. P. Flinn, R. T. Harley, M. J. Snelling, A. C. Tropper, T. M. Kerr, *Semicond. Sci. Technol.* **5**, 533 (1990); J. A. Marohn *et al.*, *Phys. Rev. Lett.* **75**, 1364 (1995); S. E. Barrett, R. Tycko, L. N. Pfeiffer, K. W. West, *ibid.* **72**, 1368 (1994); M. Krapf, G. Denninger, H. Pascher, G. Weimann, W. Schlapp, *Solid State Commun.* **78**, 459 (1991).
17. R. Hessmer *et al.*, *Phys. Rev. B* **46**, 4071 (1992).
18. C. L. Jahncke, M. A. Paesler, H. D. Hallen, *Appl. Phys. Lett.* **67**, 2483 (1995).

19. We gratefully acknowledge extended discussions with B. V. Shanabrook, Al. L. Efros, M. Rosen, and J. Yesinowski. This work was supported in part by the Office of Naval Research.

2 April 1997; accepted 15 May 1997

Identification of Maize Histone Deacetylase HD2 as an Acidic Nucleolar Phosphoprotein

Alexandra Lusser, Gerald Brosch, Adele Loidl, Hubertus Haas, Peter Loidl*

The steady state of histone acetylation is established and maintained by multiple histone acetyltransferases and deacetylases, and this steady state affects chromatin structure and function. The identification of a maize complementary DNA encoding the chromatin-bound deacetylase HD2 is reported. This protein was not homologous to the yeast *RPD3* transcriptional regulator. It was expressed throughout embryo germination in correlation with the proliferative activity of cells. Antibodies against recombinant HD2-p39 immunoprecipitated the native enzyme complex, which was composed of phosphorylated p39 subunits. Immunofluorescence microscopy and sequence homologies suggested nucleolar localization. HD2 is an acidic nucleolar phosphoprotein that might regulate ribosomal chromatin structure and function.

Posttranslational acetylation of ε-amino groups of lysines in the NH_2-terminal region of core histones has remained an enigmatic process for more than 30 years (*1*, *2*). The recent identification of histone acetyltransferase (HAT) and histone deacetylase (HD) genes as transcriptional regulators has increased our understanding of this postsynthetic modification (*3*–*9*). A mammalian HD was shown to be a homolog of the yeast *RPD3* (reduced potassium dependency) transcriptional regulator (*5*). In maize embryos, four biochemically distinct HDs have been characterized (*10*). We have recently purified maize HD2 (*11*), an enzyme with a molecular mass of about 400 kD; when denatured, HD2 splits into three polypeptides with molecular masses of 39 (p39), 42 (p42), and 45 kD (p45). Internal peptide sequences revealed that the three polypeptides are highly homologous (*11*). Oligonucleotides deduced from these sequences (Fig. 1) were used for amplification of the encoding cDNA by the reverse transcriptase–polymerase chain reaction (RT-PCR). Analysis of the complete cDNA [1121 base pairs (bp)] revealed an open reading frame

Department of Microbiology, University of Innsbruck Medical School, Fritz-Pregl-Str. 3, A-6020 Innsbruck, Austria.

*To whom correspondence should be addressed.

of 924 bp that encoded a protein of 307 amino acids with a calculated molecular mass of 33.2 kD (Fig. 1). Peptide sequences derived from p39, p42, and p45 (a total of 66 amino acids) were unambiguously identified in the cDNA sequence. The cDNA revealed a short acidic region from amino acid 97 to 111 that contained 80% Asp and Glu residues and an extended acidic region between amino acids 150 and 196 that contained 72% Asp and Glu residues.

Recombinant p39 (rHD2-p39) was fused to a His-tag, and this fusion protein migrated at an apparent molecular mass of 40 kD after SDS–polyacrylamide gel electrophoresis (SDS-PAGE) (Fig. 2A) due to the acidic region and the additional His-tag. For immunoprecipitation, we raised antibodies against rHD2-p39 (anti–rHD2-p39). As expected from the common peptide sequences of the three HD2 components, anti–rHD2-p39 detected all three polypeptides on protein immunoblots (Fig. 2A). Antibodies did not react with other maize deacetylases, like HD1-A or HD1-B (*12*).

Affinity-purified anti–rHD2-p39 immunoprecipitated HD activity from purified maize HD2 preparations. Incubation of purified HD2 with anti–rHD2-p39 and secondary antibodies resulted in immunodepletion of enzyme activity from the supernatant (Fig. 2B). With the use of anti–rHD2-p39 [immunoglobulin G (IgG)] and protein G–Sepharose, HD activity could be measured in the immunoprecipitate; no activity could be detected in the precipitate with preimmune serum or a control containing only protein G–Sepharose (Fig. 2C). Attempts to measure enzymatic activity of rHD2-p39 failed (*13*). This may be due to an incorrect protein folding, the requirement of a distinct phosphorylation pattern for the active enzyme, or the enzyme being active only when assembled as a correct complex.

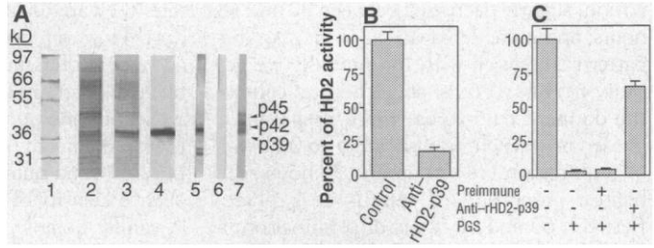

Fig. 2. (**A**) Detection of purified maize HD2 polypeptides (p39, p42, p45) by antibodies against recombinant HD2-p39. Expression and purification of HD2-p39 were done with the QIAexpressionist System (Qiagen); 5′ and 3′ ends of the HD2-p39 ORF were modified to contain a Bam HI restriction site at the 5′ end and a Hind III site at the 3′ end, by amplification with RT-PCR and cloned into the Bam HI–Hind III site of expression vector pQE9, generating a fusion protein with a His-tag. Recombinant protein was expressed in *Escherichia coli* M15[pREP4] cells and purified by Ni–nitrilotriacetic acid (NTA) agarose affinity chromatography. Coomassie blue–stained SDS-PAGE of *E. coli* extracts contained vector alone (lane 2), vector expressing His-tagged HD2-p39 (lane 3), or Ni-NTA affinity-purified rHD2-p39 (lane 4). Molecular size marker proteins are shown (lane 1). Because of the His-tag, p39 migrates at an apparent molecular mass of 40 kD. Antibodies against rHD2-p39 were raised in rabbits. rHD2-p39 (lanes 5 and 6) and purified maize HD2 (lane 7) were subjected to SDS–10% PAGE and subsequent protein immunoblotting. Blots were incubated with either purified anti–rHD2-p39 (lanes 5 and 7, dilution 1:10) or preimmune serum (lane 6) for 2 hours. Secondary antibody alkaline phosphatase conjugates were used for detection. The molecular size bands at 32 and 34 kD (lane 5) are degradation products of rHD2-p39. (**B**) Immunodepletion of HD activity. For immunodepletion, 15 μl of purified maize HD2 was incubated with 60 μl of anti–rHD2-p39 for 5 min at 25°C. Anti-rabbit IgG was added, and the immunocomplex-lattice was sedimented by centrifugation. HD activity was measured in the supernatant as described (*15*). As a control, anti–rHD2-p39 was omitted. (**C**) For immunoprecipitation, purified HD2 was incubated with 60 μl of anti–rHD2-p39 for 5 min at 25°C. Protein G–Sepharose (PGS) was added. After incubation for 1 hour at 4°C (head-over-head shaking), the beads were sedimented, washed twice with 0.5 ml of buffer B [15 mM tris-HCl (pH 7.9), 10 mM NaCl, 0.25 mM EDTA, 10 mM 2-mercaptoethanol, 10% (v/v) glycerol], and resuspended in buffer B. Control activity and samples of the precipitates were assayed for HD activity (*15*). Data are shown as the mean ± SD of four independent experiments.

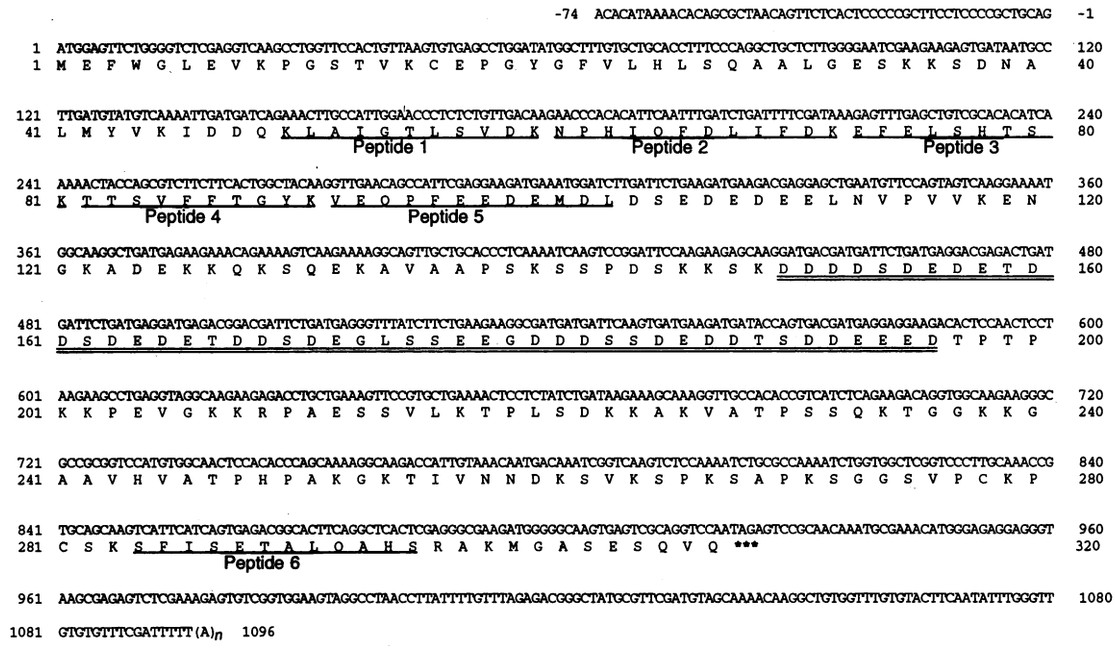

Fig. 1. Nucleotide sequence and deduced amino acid sequence of maize HD2-p39. Total maize embryo RNA was reverse transcribed. On the basis of amino acid sequences of HD2 peptides (*11*), degenerate oligonucleotide primers were designed and used for PCR amplification of cDNA fragments. PCR yielded several products that were analyzed on agarose gels, blotted, and hybridized with ^{32}P-labeled nested primers. A specific product of 112 bp was detected, cloned into pGEM-T vector (Promega), and sequenced. Subsequently, the 3′ and 5′ ends of the cDNA were amplified, subcloned, and sequenced. Peptide sequences (1 to 6), derived from protein microsequencing (*11*), are underlined. The extended acidic domain is marked (double line). The stop codon is denoted by asterisks, and the polyadenylate tail is shown as $(A)_n$. Abbreviations for the amino acid residues are as follows: A, Ala; C, Cys; D, Asp; E, Glu; F, Phe; G, Gly; H, His; I, Ile; K, Lys; L, Leu; M, Met; N, Asn; P, Pro; Q, Gln; R, Arg; S, Ser; T, Thr; V, Val; W, Trp; and Y, Tyr.

Northern (RNA) blot analysis of total RNA from different times of embryo germination with an HD2-p39 probe revealed a single transcript of about 1300 bp. This transcript was present throughout germination (Fig. 3). The mRNA steady-state level increased during the initial 30 hours of germination, slightly decreased between 30 and 48 hours, and increased again at 60 hours. This pattern correlated with the proliferative activity of embryo cells; about 80% of cells in the dormant embryo are in G_1 and enter S phase fairly synchronously at 15 to 20 hours of germination (*14*); at around 30 hours, the highest proportion of cells is in S phase. Between 60 and 72 hours of germination, a second, less synchronous S phase takes place.

Immunofluorescence microscopy of thin sections of maize embryos showed that HD2 is located in the nucleolus (Fig. 4, A and B). The nucleolus was specifically stained, whereas the rest of the nucleus remained dark. A weak speckled staining observed in the cytoplasm may have resulted from newly synthesized HD2. The nucleolar localization did not change during germination. This is consistent with previous findings that maize HD2 is always chromatin-bound, in contrast to HD1-B, which is either soluble or chromatin-associated, depending on the germination stage (*15*).

The nucleolar localization was examined with respect to sequence homology searches. Comparison of the HD2-p39 amino acid sequence with available databases revealed numerous homologies with acidic domains of nucleolar proteins. These homologies are frequently detected in database searches owing to the prevalence of the acidic domain; therefore, they are usually not found to be significant. However, with HD2-p39, the number and extent of homologies were highest among nucleolar proteins from several organisms, like nucleolins and nucleolar transcription factors (*16*). Alignment of the acidic stretches of HD2-p39 and human nucleolin indicated sequence identity of 40% over 66 amino acids. A similar homology resulted from the alignment with nucleolar transcription factors (for example *Xenopus* UBF1 and UBF2). Database searches without the acidic regions did not reveal homologs.

Our polymerase chain reaction (PCR) cloning strategy led to the isolation of one cDNA species encoding HD2-p39, whereas biochemical purification of HD2 yielded three homologous polypeptides after SDS-PAGE (*11*). To isolate the HD2 cDNAs encoding p42 and p45, we screened a λgt11 expression library containing maize whole seedling cDNA. However, we detected only three cDNA clones for p39. The presence of three HD2 polypeptides may result from posttranslational modification. We searched for putative phosphorylation sites in the HD2-p39 sequence and identified 10 potential sites for phosphorylation by casein kinase II. Furthermore, phosphatase digestion of purified HD2 resulted in a slight increase in the amount of HD2-p39 and -p42 (about 10% each) and a corresponding decrease of HD2-p45 in SDS-PAGE, supporting the idea of HD2 phosphorylation.

Next, we examined whether anti-phosphoserine would detect the HD2 polypeptides in protein immunoblots of purified HD2. HD2-p42 and -p45 reacted with the antibody (Fig. 4C, lane 3). Neither anti-phosphotyrosine nor anti-phosphothreonine reacted with the HD2 polypeptides (Fig. 4C, lanes 2 and 4). We also used casein kinase II for in vitro phosphorylation of rHD2-p39. The kinase phosphorylated rHD2-p39 in vitro and caused a shift in electrophoretic mobility in SDS-PAGE (Fig. 4C). After casein kinase II incubation, anti–rHD2-p39 detected two bands on protein immunoblots (Fig. 4C, lane 7) that corresponded to HD2-p39 and a phosphorylated product. The data indicate that HD2 is a complex assembled of p39 and its phosphorylated forms, p42 and p45.

In maize, three HATs and four HDs can be distinguished. Maize deacetylases differ from each other in their biochemical and enzymatic properties and subcellular localization (*10*, *15*). Two HDs are mod-

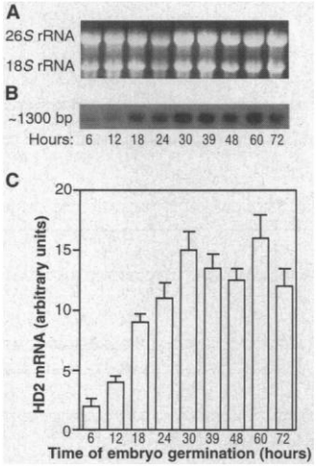

Fig. 3. Expression of HD2 mRNA during maize embryo germination. Total RNA was isolated from embryos at different times of germination, subjected to electrophoresis in 1.2% agarose, 1.1% formaldehyde gels, blotted, and hybridized with a ^{32}P-labeled 800-bp fragment of the HD2-p39 cDNA. (**A**) rRNA in an ethidium bromide–stained gel. (**B**) Autoradiogram. (**C**) The stained gel (A) and the autoradiogram (B) were evaluated quantitatively. The amount of HD2 mRNA was related to the amount of total RNA to correct for small differences in the amount of RNA loaded onto each gel slot. This ratio (labeling intensity:amount of RNA) is expressed in arbitrary units (mean ± SD of three independent experiments).

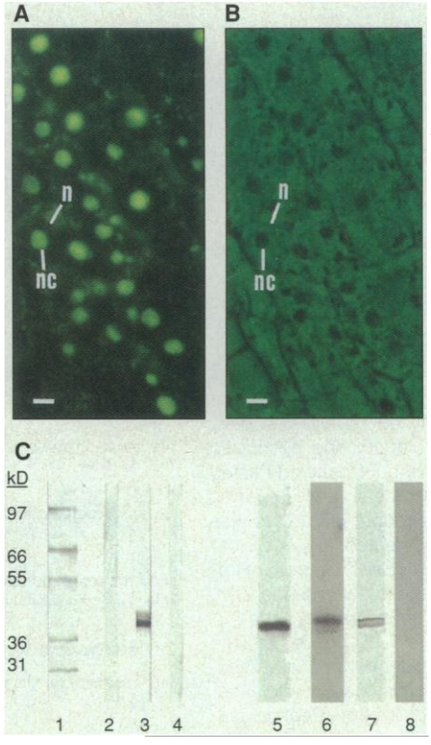

Fig. 4. Maize HD2 is located in the nucleolus. (**A**) Indirect immunofluorescence labeling (fluorescein isothiocyanate) of freeze-cut thin sections of a whole embryo at 48 hours after start of germination after incubation with anti–rHD2-p39 (2.6 mg of IgG/ml; dilution 1:100). Bar, 5 μm. (**B**) The corresponding area of (A) under phase contrast. An identical nucleolus (nc) and nucleus (n) is marked in (A) and (B). Bar, 5 μm. (**C**) Phosphorylation of HD2. Protein immunoblots of highly purified maize HD2 were analyzed with antibodies (dilution 1:250) against phosphothreonine (lane 2), phosphoserine (lane 3), and phosphotyrosine (lane 4). Lane 1, molecular size marker proteins. rHD2-p39 was phosphorylated in vitro with recombinant human casein kinase II (Calbiochem). rHD2-p39 (3 μg) was incubated with 1000 U of casein kinase II (specific activity 300,000 U/mg) in a reaction volume of 50 μl [20 mM tris-HCl (pH 7.5), 50 mM KCl, 20 mM $MgCl_2$, 200 μM [γ-^{32}P]adenosine 5′-triphosphate (ATP) (300 μCi/mmol)] at 30°C for 15 min. Products were analyzed by SDS–10% PAGE and autoradiography. To rule out the possibility of autophosphorylation of casein kinase II subunits, we performed control reactions without rHD2-p39 as substrate. rHD2-p39 was detected with anti–HD2-p39 on protein immunoblots (lane 5). After incubation with casein kinase II in vitro, phosphorylated rHD2-p39 was detected by autoradiography (lane 6). Immunoblot of lane 6 with anti–rHD2-p39 (lane 7). Casein kinase II (control) was incubated with [γ-^{32}P]ATP, but without rHD2-p39, and analyzed by autoradiography (lane 8).

ified by phosphorylation, as previously shown for HD1-A (*17*) and for HD2 in this report. A major advance in our understanding the function of histone acetylation was the identification of a mammalian deacetylase as a conserved homolog of the yeast transcriptional regulator *RPD3* (*5*). Since then, *RPD3*-homologous HDs have been identified in a variety of organisms (*6*, *18*–*20*). The identification of a maize *RPD3* homolog (*21*) and an HD that is not homologous to *RPD3* confirms the biochemical heterogeneity of maize HDs. Because HD2 is tightly chromatin-bound, located in the nucleolus, and shares homology to other nucleolar proteins, it may be involved in regulation of ribosomal chromatin structure and function by deacetylating nucleolar core histones. It is possible that enzymes for histone acetylation that are specific for ribosomal genes exist because these genes function differently in comparison to polymerase II (Pol II) genes. Ribosomal RNA (rRNA) genes are characterized by a distinct localization, a specific subset of transcriptional regulators, and a specific RNA polymerase (*22*). Moreover, rRNA is the most abundant transcript of the cell. With respect to acidic regions, HD2 shares homologies to NOR (nucleolus organizer region)-associated proteins. Proteins of this group, like RNA Pol I, nucleolin, UBF-transcription factors, and other Ag-NOR-proteins, function in rDNA transcription and are bound to ribosomal chromatin, regardless of the actual transcriptional activity. In addition, some of these proteins, like HD2, are modulated by phosphorylation (*23*).

We have previously demonstrated that HC toxin of the maize pathogen *Cochliobolus carbonum* and related cyclic tetrapeptides inhibit HDs and cause hyperacetylation of histones in susceptible, but not in resistant, maize strains (*24*). Our interpretation was that the inhibition of histone deacetylation interfered with the induction of plant defense genes. Hence, inhibition of deacetylation by HC toxin may lead to a rather general inhibition of host rDNA transcription, owing to inhibition of nucleolar HD2. Recently, the cyclic tetrapeptide apicidin was shown to inhibit protozoal HD (*25*). The antiparasitic effect was explained by the effect of HD in transcriptional control but may also be due to inhibition of rDNA replication or transcription by targeting the nucleolar HD.

Our results show that apart from *RPD3*-type HD, another nucleolar deacetylase exists. This finding confirms the multiplicity of HDs in maize and other organisms at a molecular level. The divergent functions of acetylation in nuclear processes may be reflected in multiple enzymes that differ in specificity, molecular targets, and expression in certain developmental stages.

REFERENCES AND NOTES

1. B. M. Turner, *J. Cell Sci.* **99**, 13 (1991).
2. P. Loidl, *Chromosoma* **103**, 441 (1994).
3. S. Kleff, E. D. Andrulis, C. W. Anderson, R. Sternglanz, *J. Biol. Chem.* **270**, 24674 (1995).
4. J. E. Brownell *et al.*, *Cell* **84**, 843 (1996).
5. J. Taunton, C. A. Hassig, S. L. Schreiber, *Science* **272**, 408 (1996).
6. S. E. Rundlett *et al.*, *Proc. Natl. Acad. Sci. U.S.A.* **93**, 14503 (1996).
7. V. V. Ogryzko, R. L. Schiltz, V. Russanova, B. Howard, Y. Nakatani, *Cell* **87**, 953 (1996).
8. A. J. Bannister and T. Kouzarides, *Nature* **384**, 641 (1996).
9. C. A. Mizzen *et al.*, *Cell* **87**, 1261 (1996).
10. T. Lechner *et al.*, *Biochim. Biophys. Acta* **1296**, 181 (1996).
11. G. Brosch, A. Lusser, M. Goralik-Schramel, P. Loidl, *Biochemistry* **35**, 15907 (1996).
12. T. Lechner, G. Brosch, P. Loidl, unpublished results.
13. A. Lusser and P. Loidl, unpublished results.
14. E. I. Georgieva *et al.*, *Planta* **192**, 118 (1994).
15. A. Grabher *et al.*, *Biochemistry* **33**, 14887 (1994).
16. Database searches revealed sequence similarities between HD2 and several nucleolar proteins from human, *Xenopus*, Chinese hamster, rat, and pea (for examples, GenBank accession numbers M60858, X72957, L42570, M61726, X56039, and L43510)
17. G. Brosch, E. I. Georgieva, G. López-Rodas, H. Lindner, P. Loidl, *J. Biol. Chem.* **267**, 20561 (1992).
18. J. K. Tyler, M. Bulger, R. T. Kamakaka, R. Kobayashi, J. T. Kadonaga, *Mol. Cell. Biol.* **16**, 6149 (1996).
19. W. M. Yang, C. Inouye, Y. Zeng, D. Bearss, E. Seto, *Proc. Natl. Acad. Sci. U.S.A.* **93**, 12845 (1996).
20. F. De Rubertis *et al.*, *Nature* **384**, 589 (1996).
21. T. Lechner and P. Loidl, unpublished results.
22. M. F. Trendelenburg *et al.*, *Histochem. Cell Biol.* **106**, 167 (1996).
23. R. Voit *et al.*, *EMBO J.* **11**, 2211 (1992).
24. G. Brosch, R. Ransom, T. Lechner, J. D. Walton, P. Loidl, *Plant Cell* **7**, 1941 (1995).
25. S. J. Darkin-Rattray *et al.*, *Proc. Natl. Acad. Sci. U.S.A.* **93**, 13143 (1996).

26. We are grateful to S. Grässle, P. Holzfeind, F. Marx, B. Redl, C. Seiser, and G. Stöffler for valuable discussions, and H. Feichtinger for help with maize embryo thin sections. A. Lusser is a recipient of a fellowship from the Austrian Academy of Sciences. Supported by grants from the Austrian Science Foundation (P11741), the Legerlotz-Foundation, and the Daniel-Swarovski-Foundation to P.L. The nucleotide sequence of HD2-p39 has been deposited with GenBank (accession number U82815).

27 February 1997; accepted 8 May 1997

Cellular Differentiation Regulated by Gibberellin in the *Arabidopsis thaliana pickle* Mutant

Joe Ogas,* Jin-Chen Cheng, Z. Renee Sung, Chris Somerville

The plant growth regulator gibberellin (GA) has a profound effect on shoot development and promotes developmental transitions such as flowering. Little is known about any analogous effect GA might have on root development. In a screen for mutants, *Arabidopsis* plants carrying a mutation designated *pickle* (*pkl*) were isolated in which the primary root meristem retained characteristics of embryonic tissue. Expression of this aberrant differentiation state was suppressed by GA. Root tissue from plants carrying the *pkl* mutation spontaneously regenerated new embryos and plants.

Gibberellin is required for seed germination and plays a variety of roles during growth and development after germination. GA-deficient plants exhibit defects in germination, time lag to flowering, stem elongation, apical dominance, maintenance of floral meristem identity, and trichome distribution (*1*). All of these phenotypes primarily affect the shoot. Gibberellin also affects root development by promoting cell elongation (*2*), but there is essentially no information on the effect of GA on fate determination in roots. We report here a mutant of *Arabidopsis* that is defective in a GA signaling pathway that promotes the transition of the primary root from an embryonic to an adult differentiation state.

During a screen for *Arabidopsis* mutants exhibiting abnormal root development, we identified a class of mutants in which the primary root, after a period of apparently normal growth, would thicken and become opaque and green (Fig. 1, A and B). Lateral and adventitious roots did not express this phenotype. Because of the visual appearance of the altered primary roots, we refer to this root phenotype as "pickle." Genetic analysis revealed that the mutant phenotype was due to a mutation at a single recessive locus located near position 48.4 on chromosome 2, which we named *PICKLE* (*PKL*) (*3*). Eight independent mutant alleles of the *PKL* locus have been identified by screening ~20,000 M2 plants from mutagenized populations.

Unusual cell proliferation was observed when roots were removed from mutant plants and placed on synthetic mineral me-

J. Ogas and C. Somerville, Department of Plant Biology, Carnegie Institution of Washington, 290 Panama Street, Stanford, CA 94305, USA.
J.-C. Cheng and Z. R. Sung, Department of Plant Biology, University of California, Berkeley, CA 94720–3102, USA.

*To whom correspondence should be addressed. E-mail: jogas@andrew.stanford.edu